

# Project in TMA4220

Candidatenummer: 10000 & 10028

17. November 2014

## 0.1 Poisson solver

We here present a solver for the Poisson equation,

$$\nabla^2 u = f,$$

in both 2 and 3 dimensions, with both Neumann and Dirichlet boundary conditions, while using the element method. We let  $u(r) = \sin(2\pi r^2)$  and  $f(r) = \nabla^2 u(r) = -8\pi \cos(2\pi r^2) + 16r^2 \pi^2 \sin(2\pi r^2)$ .

### 0.1.1 2D solver

The program `poisson2d.m` solves the Poisson equation in 2 dimensions, with Dirichlet boundary conditions, and created the plots in figure 1.

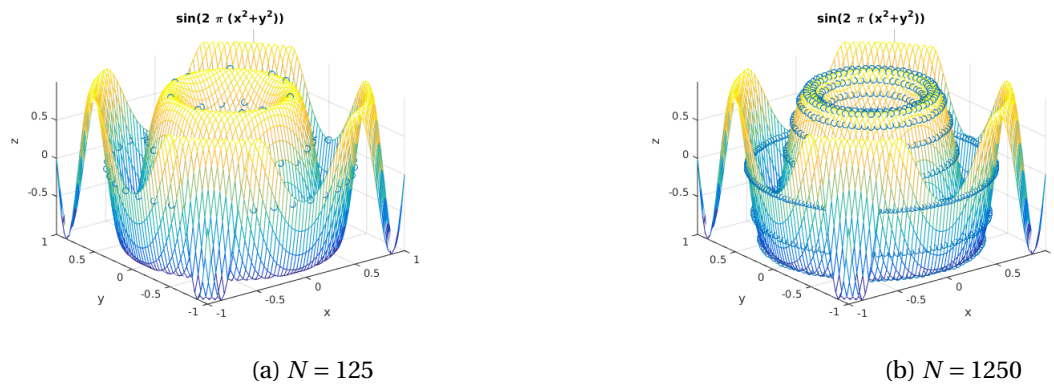


Figure 1: Scatterplots of the numerical solution of the Poisson equation in 2 dimensions, with Dirichlet boundary condition and different number of points,  $N$ , together with a surfplot of the correct solution.

The program `poissonBnd2d.m` solves the Poisson equation in 2 dimensions, with Dirichlet boundary conditions on half the domain, and Neumann on the other half, and created the plots in figure 2.

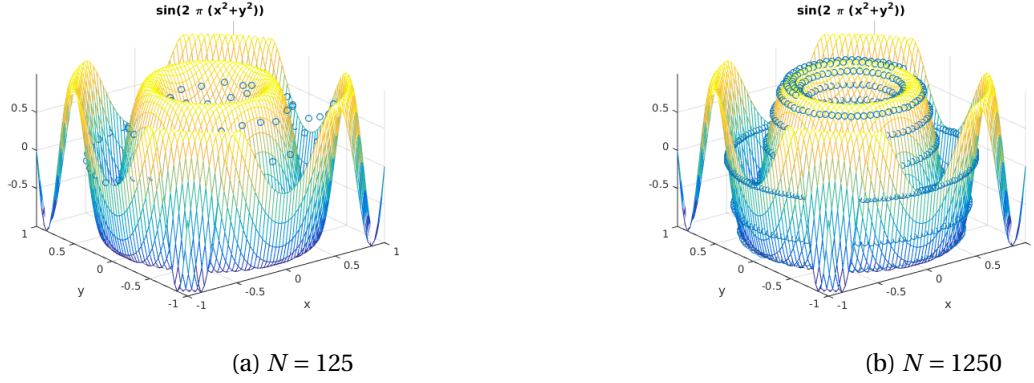


Figure 2: Scatterplots of the numerical solution of the Poisson equation in 2 dimensions, with Dirichlet boundary condition on half the boundary, and Neumann on the other half, with and different number of points,  $N$ , together with a surfplot of the correct solution.

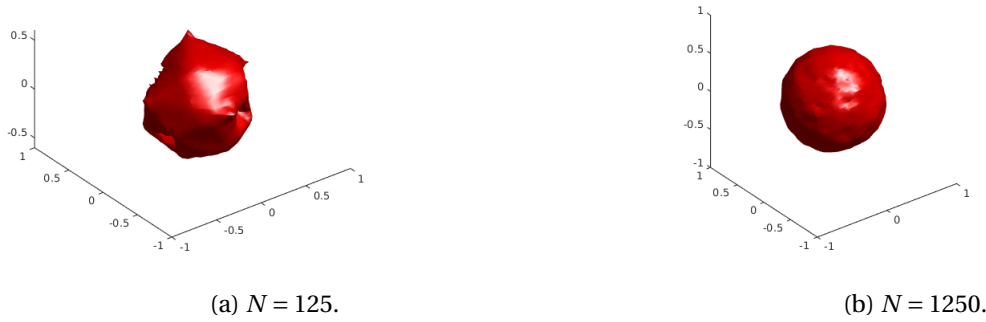


Figure 3: A plot of the numerical solution of the Poisson equation in 3 dimensions, with Dirichlet boundary condition, with different number of points,  $N$ . The correct solution is a perfect sphere.

### 0.1.2 3D solver

The program `poisson3d.m` solves the Poisson equation in 3 dimensions, with Dirichlet boundary conditions, and created the plots in figure 3.

The program `poissonBnd3d.m` solves the Poisson equation in 3 dimensions, with Dirichlet boundary condition on half the boundary, and Neumann on the other half, and created the plots in figure 4

### 0.1.3 Discussion

As we can see from figure 1 and figure 2, the 2 dimensional case works quite good, and seems to be convergent. Thus `poisson2d.m` and `poissonBnd2d.m` are working solvers for the Poisson equation.

Also the 3 dimensional case with Dirichelt boundary the solver `poisson3d.m` converges. But when including the Neumann boundary condition the  $A$  matrix became singular because we needed to include

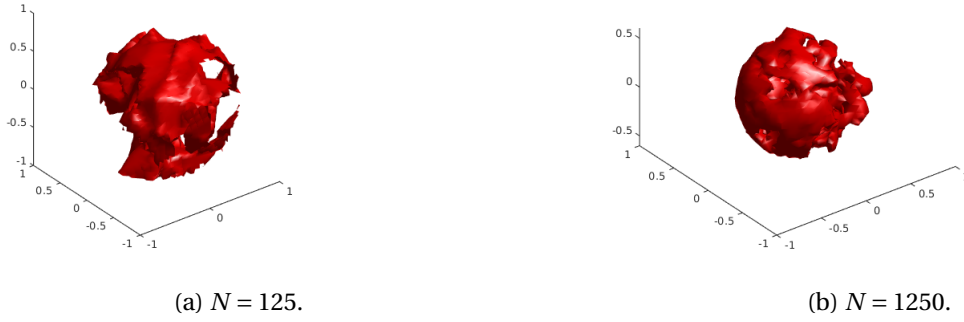


Figure 4: A plot of the numerical solution of the Poisson equation in 3 dimensions, with Dirichlet boundary condition on half the boundary, and Neumann on the other half, with different number of points,  $N$ . The correct solution is a perfect sphere.

some points on the boundary which we did not need while only having Dirichlet boundary. There also seems to be a problem with while adding the Neumann conditions to b. Thus we conclude that the program `poisson3dBnd.m` does not work correctly. We have no clue why the Neumann conditions works in 2 dimension and not in 3 dimensions, considering that the implementation is almost identical.

## 0.2 Heat equation

We are here going to present a solution to the heat equation in 3 dimensions using Neumann conditions on the edges, with forward Euler in time, and element-method in space.

### 0.2.1 Weak formulation

The heat equation

$$\frac{\partial u}{\partial t} = \alpha \nabla^2 u \quad (1)$$

Using *Greens formula* we obtain

$$\int_{\Omega} \frac{\partial u(\mathbf{x})}{\partial t} v(\mathbf{x}) d\Omega = \int_{\Omega} \Delta u(\mathbf{x}) v(\mathbf{x}) d\Omega = - \int_{\Omega} \nabla u(\mathbf{x}) \nabla v(\mathbf{x}) d\Omega + \int_{\Gamma} \frac{\partial u}{\partial n}(\mathbf{x}) v(\mathbf{x}) d\gamma.$$

This has an unique solution if continuous and weakly coercive.  $f \equiv 0$  for our equation.

The scheme is weakly coercive if  $a(u, u) + \lambda \|u\|_{L^2(\Omega)}^2 \geq \alpha \|u\|_V^2$  for  $\lambda \geq 0, \alpha > 0$ , with  $a(u, v) = \int \nabla u(\mathbf{x}) \nabla v(\mathbf{x}) d\Omega$ .

$|a(u, v)| = |\int \nabla u \nabla v d\Omega| \leq \sqrt{\int (\nabla u)^2 d\Omega} \sqrt{\int (\nabla v)^2 d\Omega} = \|u\|_V \|v\|_V$  so the the scheme is continuous.

$|a(v, v)| = \int \nabla v \nabla v d\Omega = \|v\|_V^2$ , so this scheme is weakly coercive for  $\alpha \leq 1$ . Therefore there exists a unique solution.

Trying to solve our problem using  $v$  and  $u$  in the space  $H^1(\Omega)$ , approximated by  $X_h^1 = \{v_h \in C^0(\bar{\Omega}) : v_h|_K \in \mathbb{P}_1 \forall K \in \tau_h\}$  in both 2 and 3 dimensions.  $V_h = \{v_h \in X_h^1 : v \text{ satisfying boundary conditions}\}$ . Using Lagrangian functions  $\phi_j \in V_h$  with the property

$$\phi_j(x_i) = \delta_{ij} = \begin{cases} 1 & i = j \\ 0 & i \neq j \end{cases}$$

### 0.2.2 Galerkin

We can make a Galerkin problem using

$$u_h(\mathbf{x}, t) = \sum_{j=1}^{N_h} u_j(t) \phi_j(\mathbf{x}) \text{ and } v \in \text{span}\{\phi_1, \phi_2, \dots, \phi_{N_h}\}.$$

This gives

$$\begin{aligned} \int \sum_{j=1}^{N_h} \frac{\partial u_j}{\partial t} \phi_j \phi_i d\Omega + a\left(\sum_{j=1}^{N_h} u_j(t) \phi_j, \phi_i\right) &= \int_{\Gamma} \sum_{j=1}^{N_h} \frac{\partial u_j(t) \phi_j}{\partial n} \phi_i d\gamma \\ \sum_{j=1}^{N_h} \frac{\partial u_j}{\partial t} \int \phi_j \phi_i d\Omega + \sum_{j=1}^{N_h} u_j(t) a(\phi_j, \phi_i) &= \sum_{j=1}^{N_h} \frac{\partial u_j}{\partial t} m_{ij} + \sum_{j=1}^{N_h} u_j(t) a_{ij} = b_i \end{aligned}$$

This is the linear system,  $M\dot{\mathbf{u}}(t) + \mathbf{A}\mathbf{u}(t) = \mathbf{0}$ , the boundary conditions get inserted differently.

The Lagrangian functions  $\phi$  is on the form  $\phi_i = \alpha_i x \beta_i y + \gamma_i$ . For  $K_j$   $\phi_i$  is 1 in  $(x, y) = (x_i, y_i)$  and 0 in the other corners in  $K$ . The  $K$  elements are triangles in 2 dimensions and tetrahedrons in 3 dimensions, and together they cover our domain  $\Omega$ .

The Galerkin method let's us finally construct forward Euler method iterations on the form  $M \frac{\mathbf{u}^{k+1} - \mathbf{u}^k}{\Delta t} + \mathbf{A}\mathbf{u}^k = \mathbf{0}$ .

### 0.2.3 Stability of forward euler galerkin

The stability analysis for forward euler in time and FEM in space we find by using  $w_h^j$  which is eigenvectors of  $a(\cdot, \cdot)$  instead of  $\phi$ , the step-size  $h$  may vary in space.

$$\frac{1}{\Delta t} \sum_{j=1}^{N_h} [u_j^{k+1} - u_j^k] \int w_h^j w_h^i + \sum_{j=1}^{N_h} u_j^k a(w_h^j, w_h^i) = 0$$

The eigenvalues of the matrix can be calculated

$$a(w_h^j, w_h^i) = \int \nabla w_h^j \nabla w_h^i d\Omega = \lambda_h^j \int w_h^j w_h^i d\Omega = \lambda_h^j (w_h^j, w_h^i) = \lambda_h^j \delta_{ij} = \lambda_h^i$$

giving

$$\frac{u_j^{k+1} - u_j^k}{\Delta t} + u_j^k \lambda_h^i = 0 \Rightarrow u_j^{k+1} = u_j^k (1 - \lambda_h^j \Delta t).$$

For the method to be absolutely stable we need  $|1 - \lambda_h^j \Delta t| < 1$ .

$-1 < 1 - \lambda_h^j \Delta t < 1 \Rightarrow 0 < \Delta t < \frac{2}{\lambda_h^i}$ . The eigenvalues for the stiffness matrix are

$$\max_i \lambda_h^i = \max_i \frac{a(w_h^i, w_h^i)}{\|w_h^i\|_{L^2(\Omega)}^2} \leq \max_i \frac{\|w_h^i\|_V^2}{\|w_h^i\|_{L^2(\Omega)}^2} \simeq (1 + \frac{c}{h^2}), \text{ since } \|\nabla u\|_{L^2(\Omega)} \leq \frac{C\|u\|_{L^2(\Omega)}}{h}.$$

We get that this method only is stable if  $\Delta t \leq Ch^2$ .

## 0.2.4 Initial and boundary conditions

We assume that the body initially has a uniform temperature,  $T_i$ .

On the boundary we have Neumann-conditions. We divide the boundary in two parts,  $\partial\Omega_H$ ,  $\partial\Omega_C$ .  $\partial\Omega_H$  is the part of the boundary that is in contact with temperature  $T_H$ , while  $\partial\Omega_C$  is in contact with temperature  $T_C$ .

## 0.2.5 Numerical scheme

The resulting equations that needs to be solved is

$$\begin{aligned} M \frac{du}{dt} &= -\alpha A u && \text{on } \Omega \\ \frac{\partial u}{\partial \nu} &= \alpha_H (T_H - u) && \text{on } \partial\Omega_H \\ \frac{\partial u}{\partial \nu} &= \alpha_C (T_C - u) && \text{on } \partial\Omega_C. \end{aligned}$$

This is a simple set of ODEs, and is solved using forward Euler. The numerical scheme can then be written as

$$\begin{aligned}
u^{i+1} &= u^i - \alpha(M \setminus A)u^i && \text{on } \Omega \\
u^{i+1} &= u^i + \alpha_H(T_H - u^i) && \text{on } \partial\Omega_H \text{ .} \\
u^{i+1} &= u^i + \alpha_C(T_C - u^i) && \text{on } \partial\Omega_C
\end{aligned}$$

Where  $\alpha$ ,  $\alpha_H$  and  $\alpha_C$  are the heat conductivity in the body, heat conductivity between  $\partial\Omega_H$  and  $T_H$ , the heat conductivity between  $\partial\Omega_C$  and  $T_C$ , respectively.

### 0.2.6 Correctness of Method

To test if  $A$ ,  $b$  and  $M$  where correct, we wanted to find

$$\begin{aligned}
E_A &= \|Au - b_1\|_2, & b_1 &= \int_{\Omega} f v d\Omega \\
E_M &= \|Mu - b_2\|_2, & b_2 &= \int_{\Omega} u v d\Omega
\end{aligned}$$

with  $u(r) = \sin(2\pi r^2)$ ,  $f(r) = \nabla^2 u(r) = -8\pi \cos(2\pi r^2) + 16r^2\pi^2 \sin(2\pi r^2)$  on the unit sphere. The program `error3d.m` was made for this purpose, and produced tabel 1, and figure 5. From table 1 it seems that  $E_A$  does not converge, but some experimentation with `error3d.m` shows that it decreases extremely slowly with increasing  $N$ . For the matrix  $M$  this is not an issue and it converges nicely. The 2 dimensional case will not be discussed in this report, but the program `error2d.m` can be used if this is of interest.

### 0.2.7 Example of use

As an example of use we wanted to cook a beef. For that we need a lot of different assumptions.

- The beef has a initial uniform temperature  $T_i = 10^\circ C$ , and is turned when the temperature on the middle poit reaches a temperature  $T_f = 60^\circ C$ . It is done when the lowest temperature in the beef is  $T_f = 60^\circ C$ .  $T_H = 180^\circ C$ ,  $T_C = 20^\circ C$ .
- The beef is discretized with  $n_1 = n_2 = n_3 = 5$  with the function `getbeef.m`.
- Thermal conductivities are independant of temperature, and as follows:  
 $\alpha = 8.75 \cdot 10^{-8}$ ,  $\alpha_H = 0.7$ ,  $\alpha_C = 3 \cdot 10^{-4}$ .

#	$N = 125$	$N = 250$	$N = 1250$
$E_A$	19.50	22.09	12.82
$E_M$	0.1165	0.0556	0.0121

Table 1: Error of  $A$  and  $M$ , when compared to their corresponding  $b_1$  and  $b_2$ .

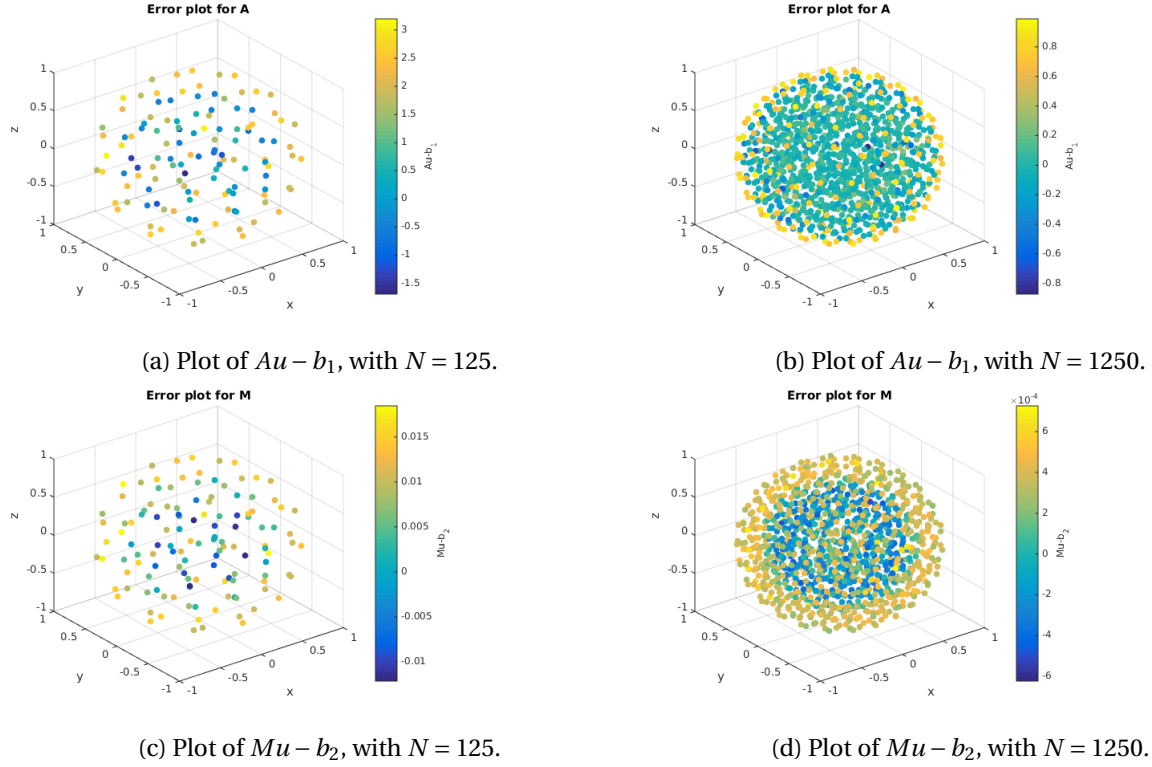


Figure 5: A scatterplott showing the pointwise error of  $A$  and  $M$ , with different number of points,  $N$ .

$\alpha$  is given in the task,  $\alpha_H$  is assumed to be quite large, while  $\alpha_C$  is assumed to be somewhere in between  $\alpha$  and  $\alpha_H$ . The other constants are chosen freely.

## Result

Running the program `beef.m` with these assumptions, gives out the following times:

- Time to turn the beef: 658 seconds
- Total time to the beef is done: 776 seconds

This is close to 13 minutes in total cookingtime, which seems about right for a normal steak. As we can see from figure 6, the edges are all cooked, while the upper middle is some what raw.

## Discussion

Although the program `beef.m` gives a time-estimate similar to the reality, it is in no way an accurate description. The numerical scheme has it problems, the  $A$  matrix converges extremely slow with  $N$ . The program gives different cookingtime with differnet values of  $n_i$ .

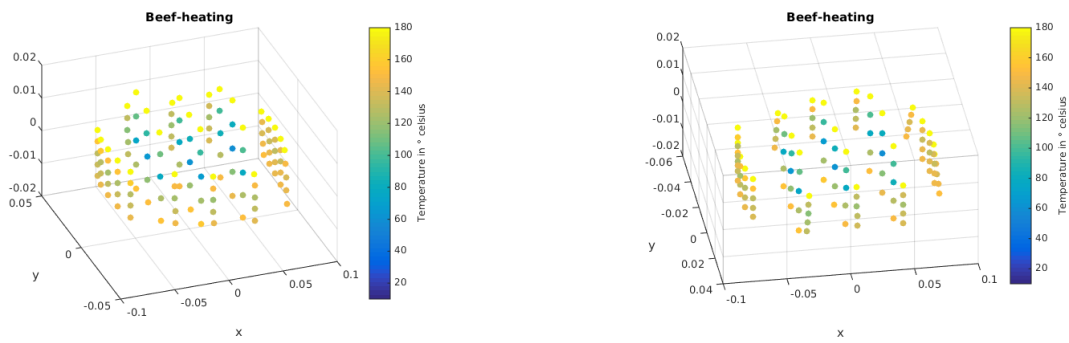


Figure 6: A scatterplott of a cooked beef from two different angles.